PART 1

The Modern setting

1

Upwelling processes associated with Western Boundary Currents

L. PIETRAFESA

Abstract

Upwelling processes associated with Western Boundary Currents (WBCs) include not only classical wind driven coastal upwelling but also mechanisms due to buoyancy flux, topography and boundary current frontal instabilities. Sharp breaks in cross-shelf bottom topography can create localized transient pockets of uplifted isopycnals during occasions of wind-forced upwelling events. Longshore variations in bathymetry interacting with a WBC can have the effect of torquing the sheared jet across isobaths and kinematically inducing upwelling, creating regions of persistent or quasi-permanent upwelling. Isolated topographic ridges or bumps, such as the Charleston Bump, a topographic rise sitting atop the continental slope directly in the path of the Gulf Stream can cause WBCs to deflect offshore creating a downstream wave trough which, via bottom Ekman suction, can support a continental slope region of persistent upwelling. WBCs are characterized by frontal instabilities which manifest themselves as shelf-break hugging, downstream-propogating frontal meanders and filaments. These features are found to be responsible for creating shelf-break upwelling domes and ridges. These events can act occasionally in concert with wind and buoyancy stress-forcing to create shelf-wide upwelling. All of the above WBC related upwelling processes are shown to be important to the supply of high concentrations of phosphate to local continental margin and shelf regions. Relatively high values of phosphate are shown to exist where the upwelling processes described above are present in WBC systems, such as the Gulf Stream.

Introduction

In the classic standard entitled *Upwelling* by R.L. Smith (1968), the following description of the 'phosphate' distribution is given:

> Phosphate, or dissolved inorganic phosphorous, generally increases with depth from very low values at the surface to maximum values at some intermediate depth. It is one of the principal nutrients and therefore important to life in the sea. High values occur in upwelling regions where subsurface water comes to the surface. The usual mid-latitude oceanic surface concentration is of the order of 0.2 μg-atom/l. In the upwelling regions of Peru (Posner, 1957) and the Benguela Current (Hart & Currie, 1960) the surface concentration is between 1 and 2 μg-atom/l. Values of over 2 μg-atom/l were found at the surface of the south-east Arabian coast (Royal Society, 1963), and Laurs (1967) has reported values of 2.5 μg-atom/l near the coast during intensive upwelling off Oregon.

It appears clear that values of phosphates which make for the importance of 'upwelling' as a physical process in supplying dissolved inorganic phosphorous to continental margin regions are 1–2.5 μg-atom/l versus ambient values of an order of magnitude less. What is upwelling?

Smith (1968) defines upwelling as 'an ascending motion, of some minimum duration and extent, by which water from subsurface layers is brought into the surface layer'. Smith points out that while the word 'upwelling' has been used extensively throughout oceanography, dating back to Sverdrup (1938), a precise definition had not been coined prior to Smith (1968). Since the Smith summary, much has been written about the physical, biological and chemical oceanography of coastal upwelling zones. The importance of these zones was further emphasized by Ryther (1969). He estimated that fully one-half of the world's fish food supply is derived from upwelling regions.

A recent survey publication entitled *Coastal Upwelling* (Richards, 1981) documents the new knowledge derived from such major programs as the National Science Foundation – International Decade of Ocean Exploration Coastal Upwelling Ecosystems Analysis. These programs have provided much new insight into the interrelationships between the physics and biology of wind-driven upwelling systems such as are found along the Pacific coasts of the United States and South America, and the Atlantic coasts of North and South Africa. These are all eastern boundaries of ocean basins (cf. Fig. 1.1). However, few studies were made of upwelling regions and mechanisms which might exist along the western sides of ocean basins.

Smith (1968) states that 'the major atmospheric systems' indigenous to the eastern sides of ocean basins 'are favorable to upwelling over extended areas and periods'. He also notes that 'upwelling of more limited extent can be found elsewhere, when and where the local winds transport water in the surface layer offshore'. Smith alludes to several reports of upwelling along the northeastern coast of Florida (Green, 1944; Taylor & Stewart, 1959), North Carolina (Wells & Gray, 1960) and on the Caribbean coast of Venezuela (Richards, 1960). So, by 1968 there was some testimony, albeit minimal, concerning the occurrences of

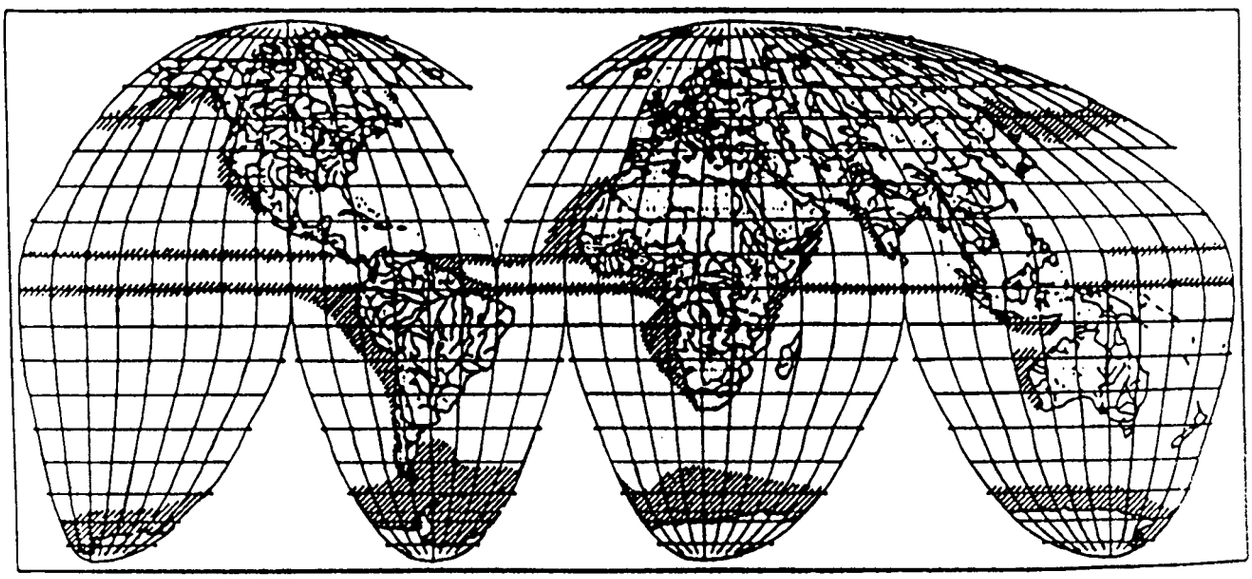

Fig. 1.1. General world areas of upwelling which are also areas of high organic production (Fairbridge, 1966).

upwelling along the western sides of ocean basins. The important note here is that strong, longshore Western Boundary Currents (WBCs) occur on the western sides of ocean basins, and where upwelling is present in these regions, such processes could be associated with the presence of the WBCs.

Even if upwelling were to occur along western sides of ocean basins, is there enough evidence that phosphate is present in the water columns of such regimes to justify an interrogation of the dynamics? In a US Department of the Interior literature survey of the National Oceanographic Data Center's records of the observed distribution of oceanic variables along the continental margin of the southeastern seaboard of the continental United States (ERT, 1979a,b) the following statement is made:

> Most high phosphate concentrations (>0.5 μg-atom/l) occur in the lower part of the water column over the shelf break region . . . Relatively high mid-shelf and near-shore values are occasionally noted both at the surface and near the bottom in various sections and in various seasons.

Thus, as of 1978, there was evidence of 'relatively high' phosphate occurring in the South Atlantic Bight (Fig. 1.2), the western boundary current region of the southeastern continental USA. Herein, Atkinson, Pietrafesa & Hoffman (1982), provided the pictoral, diagrammatic relationships between water column temperature/nitrate/phosphate values shown in Figure 1.3 for the region between Capes Fear and Hatteras, NC (Fig. 1.4). Clearly, as shown in Figure 1.3, phosphate concentrations of 1–2 μg-atom/l are not uncommon in these waters. Could the occurrences of high phosphate in North Carolina coastal waters be related to upwelling phenomena?

Recently, investigators such as Pietrafesa & Janowitz, (1979), Hofmann *et al.*, (1980), Janowitz & Pietrafesa, (1980), Pietrafesa & Janowitz, (1980), Blanton *et al.*, (1981), Hofmann, Pietrafesa & Atkinson, (1981), Leming & Mooers (1981), Atkinson, Pietrafesa & Hofmann, (1982), Janowitz & Pietrafesa, (1982), McClain, Pietrafesa, & Yoder, (1984) and Pietrafesa, Janowitz & Wittman, (1985) have discussed a variety of upwelling processes which occur in the South Atlantic Bight (SAB) of the USA. The SAB is the continental margin region between Cape Canaveral, Florida and Cape Hatteras, NC (Figs. 1.2, 1.3). It is likely that similar phenomena are present along other western oceanic boundaries, such as the western Pacific and the Mid-Atlantic Bight of the USA, South America and Africa. We shall discuss the upwelling mechanisms which can be present along western boundaries of ocean basins, test their application to a specific locale, the SAB, and make inferences for similar regions of the world's oceans.

Upwelling theory

Consider the classical balance relations in a form conventionally used in oceanographic applications (for a complete derivation refer to Fofonoff, 1962):

(a) (b) (c) (d) (e) (f)

$$\frac{Du}{Dt} = fv - \alpha\frac{\partial P}{\partial x} + \frac{\partial}{\partial x}\left(A_x\frac{\partial u}{\partial x}\right) + \frac{\partial}{\partial y}\left(A_y\frac{\partial u}{\partial y}\right) + \frac{\partial}{\partial z}\left(A_z\frac{\partial u}{\partial z}\right) \quad (1.1)$$

(g) (h) (i) (j) (k) (l)

$$\frac{Dv}{Dt} = fv - \alpha\frac{\partial P}{\partial y} + \frac{\partial}{\partial x}\left(A_x\frac{\partial v}{\partial x}\right) + \frac{\partial}{\partial y}\left(A_y\frac{\partial v}{\partial y}\right) + \frac{\partial}{\partial z}\left(A_z\frac{\partial v}{\partial z}\right) \quad (1.2)$$

(m) (n)

$$\frac{\partial P}{\partial z} = -g\rho \quad (1.3)$$

(o) (p) (q)

$$\frac{\partial u}{\partial x} + \frac{\partial v}{\partial y} + \frac{\partial w}{\partial z} = 0 \quad (1.4)$$

(r) (s) (t) (u)

$$\frac{D\rho}{Dt} = \frac{\partial}{\partial x}\left(K_x\frac{\partial \rho}{\partial x}\right) + \frac{\partial}{\partial y}\left(K_y\frac{\partial \rho}{\partial y}\right) + \frac{\partial}{\partial z}\left(K_z\frac{\partial \rho}{\partial z}\right) \quad (1.5)$$

(v) (w) (x) (y)

$$\frac{D}{Dt} = \frac{\partial}{\partial t} + u\frac{\partial}{\partial x} + v\frac{\partial}{\partial y} + w\frac{\partial}{\partial z} \quad (1.6)$$

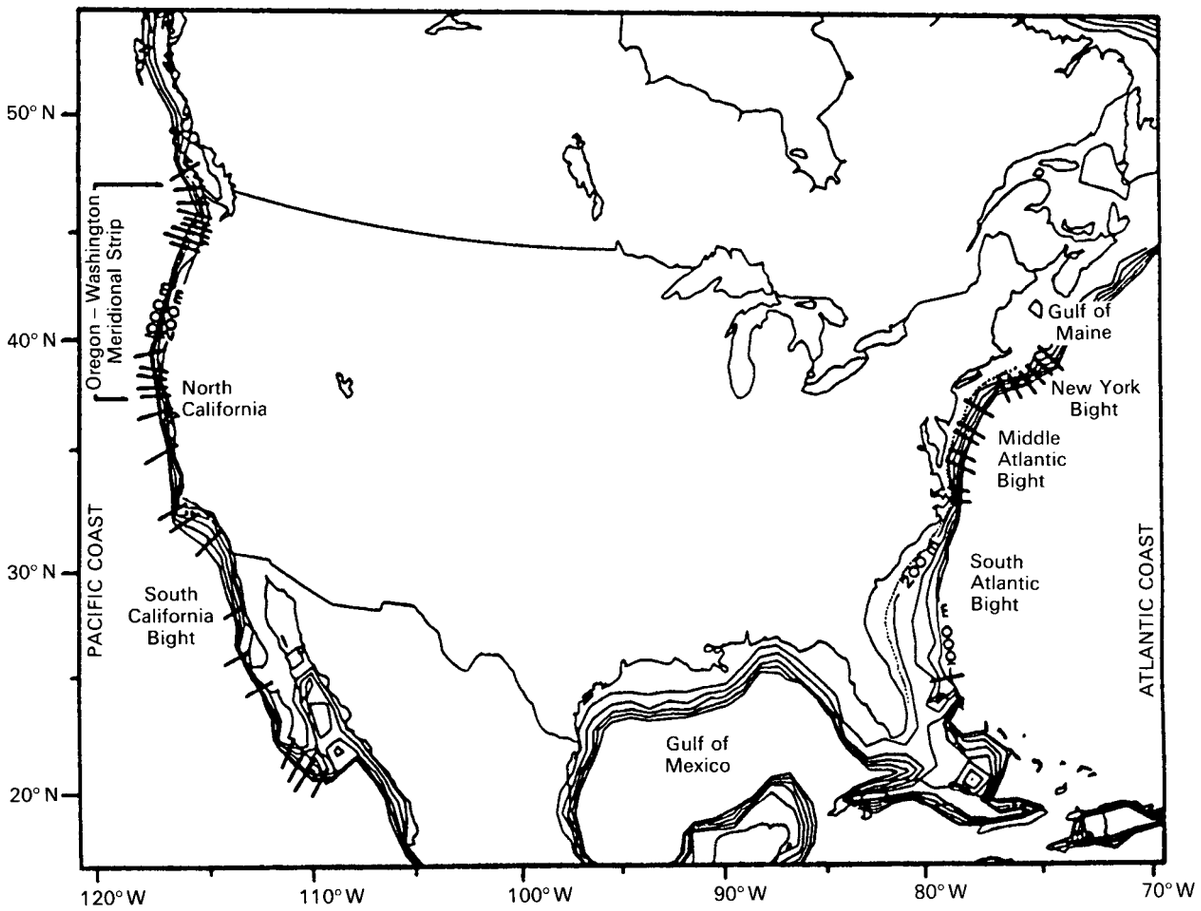

Fig. 1.2. Mainland United States continental margin regions. Submarine (continental slope) canyons are noted as straight-line cuts across the continental margins.

where u, v, w are the offshore (+x), alongshore (+y) and upwards (+z), right-handed Cartesian coordinate components of the Eulerian velocity of a water parcel, t is time, f is the Coriolis parameter ($2\Omega\sin\theta$), α is the specific volume of sea water, ρ is the density of sea water, P is pressure and the A's are eddy viscocity coefficients and the K's, the eddy diffusion counterparts in the x, y and z directions. Ω is the Earth's angular velocity and θ is latitude.

Equations (1.1) and (1.2) relate the relative acceleration of a water parcel, in the cross-shelf (or diabathic) and alongshelf (or parabathic) directions, respectively, as a function of time and space (via definition (b)) to the effect of the Earth's rotation, pressure gradient forces, and horizontal and vertical frictional forces. Relation (1.3) states the hydrostatic balance, while equations (1.4) and (1.5) provide for the conservation of volume and mass and for the distribution of the thermohaline field as well as its disposition as a forcing function.

Take equations (1.1) and (1.2), cross-differentiate them, and subtract the resulting relations, i.e. form the vectoral 'curl', while assuming that $(\partial v/\partial x - \partial u/\partial y) \ll f$ (the low Rossby number assumption). Next, combine this 'curl' relation with equation (1.4) to yield

$$\underset{(a)}{\frac{\partial w}{\partial z}} = \underset{(b)}{\frac{1}{f}\left(\frac{\mathrm{D}}{\mathrm{D}t}\right.\left.\frac{\partial v}{\partial x}\frac{\partial u}{\partial y}\right)} + \underset{(c)}{\beta v} + \underset{(d)}{\frac{\partial \alpha}{\partial x}\frac{\partial P}{\partial y}} - \underset{(e)}{\frac{\partial \alpha}{\partial y}\frac{\partial P}{\partial x}}$$
$$- \underset{(f)}{\frac{\partial}{\partial y}\left(\frac{\partial}{\partial x}\left(A_x\frac{\partial u}{\partial x}\right)\right)} + \underset{(g)}{\frac{\partial}{\partial y}\left(A_y\frac{\partial u}{\partial y}\right)} + \underset{(h)}{\frac{\partial}{\partial z}\left(A_z\frac{\partial u}{\partial z}\right)}$$
$$+ \underset{(i)}{\frac{\partial}{\partial x}\left(\frac{\partial}{\partial x}\left(A_x\frac{\partial v}{\partial x}\right)\right)} + \underset{(j)}{\frac{\partial}{\partial y}\left(A_y\frac{\partial v}{\partial y}\right)} + \underset{(k)}{\frac{\partial}{\partial z}\left(A_z\frac{\partial v}{\partial z}\right)} \quad (1.7)$$

In summary, the vertical gradient of the vertical velocity w, is related to the change in the vertical component of the relative vorticity following a water parcel, plus the meridional advection of planetary vorticity, the effects of the solenoidal pressure-density fields (which vanish in the Bousinesq limit), and the effects of the horizontal and vertical diffusion of relative vorticity.

In the classical Ekman (1905) and Sverdrup (1938) pictures of upwelling, an alongshore longshore wind blowing with a coastline to its left in the northern hemisphere would drive surface waters seaward with a transport equal to the magnitude

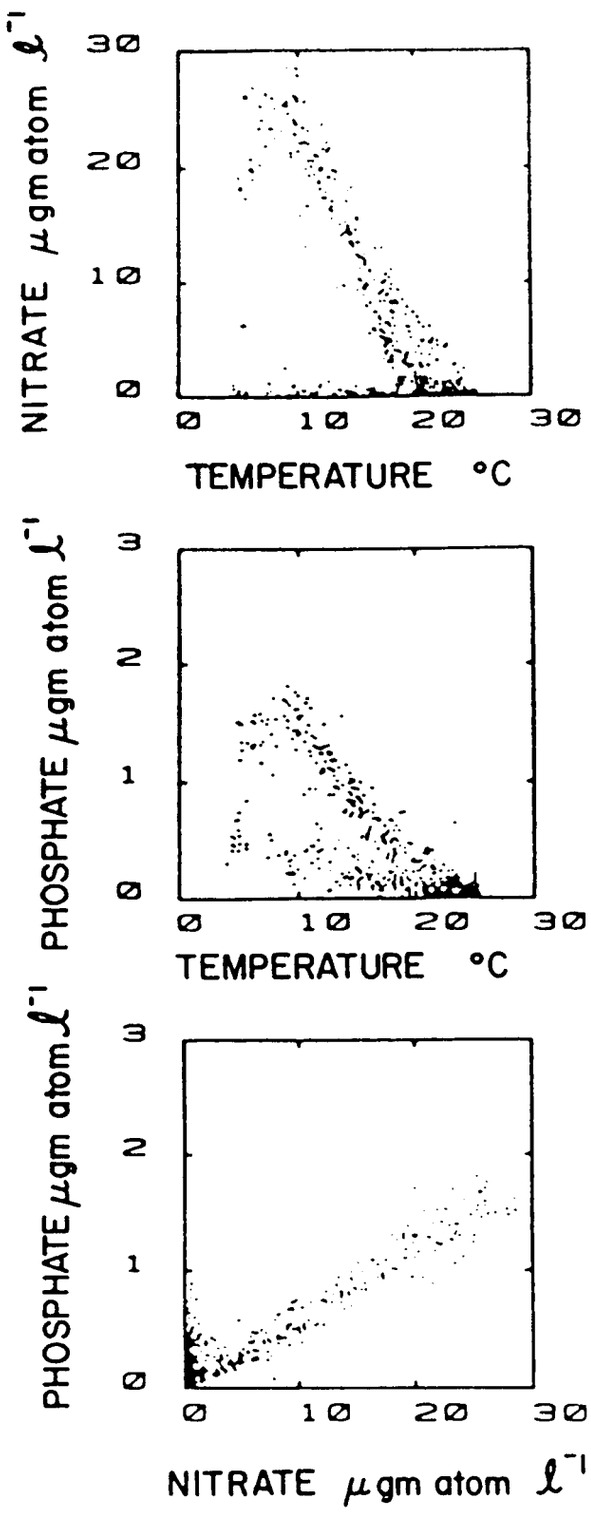

Fig. 1.3. Temperature, nitrate and phosphate relationships for outer Carolina Cape bay waters (Atkinson, Pietrafesa & Hofmann, 1982).

of the alongshore wind stress $\tau(y)$ divided by the Coriolis parameter, f. The important balance in equation (1.7) for both the Ekman and Sverdrup models is that between terms (a), (h) and (k). If a vertical integral of terms (a), (h) and (k) is formed with the conditions that a rigid lid rests on the surface of the fluid and no bottom stress is effected then a non-zero positive wind stress will be balanced by a vertically finite upwards-moving flow.

Hidaka (1954) considered model balances for equations (1.1) and (1.2) of terms (a), (b), (c), (d), (f) and (g), (h), (j), (l), separately and resolved that coastal upwelling extends a distance of $(A_x/f)^{1/2}$ from the coastline, in concert with a longshore geostrophic interior-current flowing in the direction of the wind. Garvine (1971) added the longshore pressure gradient, term (i) (eqn 1.2), to Hidaka's model and showed that the resupply of mass to the system could occur in the interior, driven geostrophically by the sea-surface tilt which is set up in the direction in which the wind is blowing rather than in a bottom layer driven by bottom stress. Garvine (1972) also introduced a linearly-sloped finite bottom and found that shallower depths result in augmented near-bottom onshore flow and stronger longshore flow. This is the first evidence of the effects of bottom topography on upwelling.

Hsueh & O'Brien (1971) considered the problem of non-wind forced upwelling by concluding that a longshore geostrophic current, located at the shelf break and flowing with the coastline to its left will necessarily result in a bottom-layer flow onto the shelf. Hsueh & O'Brien defined this to be 'current induced upwelling'. This mechanism of driving coastal upwelling, without an 'upwelling favorable' surface wind was an important finding; a boundary current could drive coastal upwelling.

Arthur (1965) and Yoshida (1967) both considered lateral topographic effects via balances of terms (a), (b) and (c) in equation (1.7). The argument is that as a longshore current flows by a wall to its left, if a cape appears, i.e. if the wall 'moves away' from the current, then a cyclonic vortex will form in the lee of the cape and upwelling will occur in the center of the vortex. This mechanism must be treated judiciously because, in the inviscid limit, over a flat bottom, under a rigid lid, on an f-plane, the vertical velocity is identically zero, since the material derivative of the potential vorticity is equal to a zero. Terms (h) and (k) can provide for vertical motions driven by both the curl of the wind stress and the curl of bottom stress but these effects can only be estimated given the paucity of atmospheric wind data collected serially from meteorological buoys and given very few bottom stress estimates based on observations.

In all of the aforementioned models, a key ingredient missing from consideration was stratification. As indicated by equations (1.5) and (1.7), upwelling is a non-linear coupled process. The degree of non-linearity or of baroclinic effect is moot; the point is that the system is coupled via the strong stratification associated with upwelling. The studies of Charney (1955), Lineykin (1955), Yoshida (1967), Tomczak (1970), Leetma (1971), Allen (1972 and 1973), Blumsack (1972), Hsueh & Kenney (1972), O'Brien & Hurlburt (1972), Hurlburt & Thompson (1973), McNider & O'Brien (1973), Pietrafesa (1973), Thompson & O'Brien (1973), Pietrafesa & Janowitz (1979), all incorporated the effects of stratification and were able to deduce many of the more salient features of the upwelling process, as discussed by Mooers, Col-

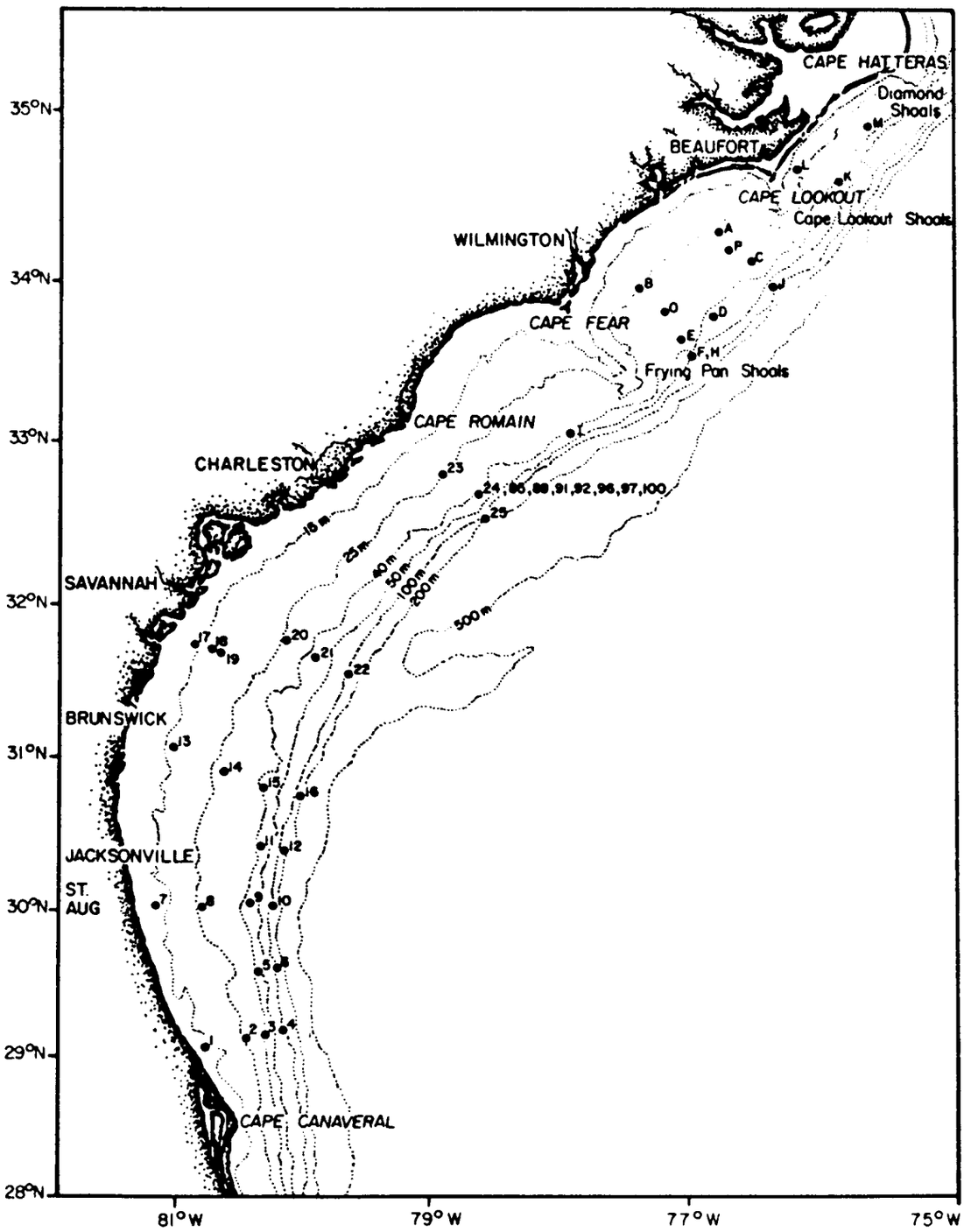

Fig. 1.4. South Atlantic Bight plus North Carolina State University and University of Miami current meter moorings, 1975–81.

lins & Smith (1976). Several important length scales were derived from these studies; they include an horizontal length scale, measured from the coastline seaward, within which 'coastal' upwelling is confined. It is the baroclinic radius of deformation and for a two-layer fluid is equal to $((\rho_2-\rho_1)gh_1h_2/\rho_2 f^2(h_1+h_2))^{1/2}$ where h_1, and h_2 are upper and lower layer thicknesses, and ρ_1 and ρ_2 are upper and lower layer densities.

Prior to 1972, only wind forcing was considered to be important as a surface forcing mechanism of continental margin upwelling, but Stommel & Leetma (1972), Pietrafesa (1973) and Pietrafesa & Janowitz (1979) considered the effects of thermohaline processes, via buoyancy flux 'stress' and pressure gradients. Included in these effects are such features as outwelling estuarine plumes, horizontal density differences from

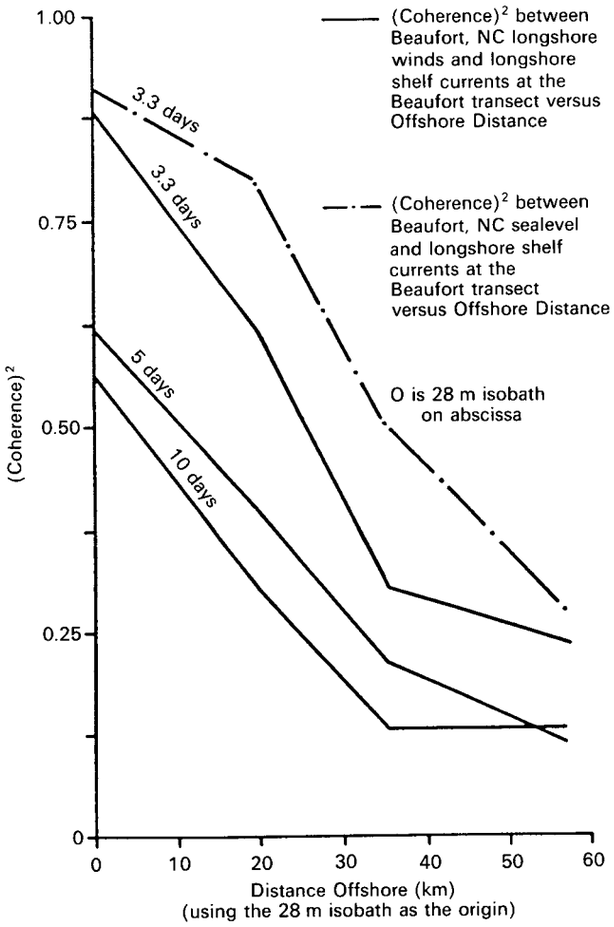

Fig. 1.5. (Coherence)² between Beaufort longshore winds and longshore shelf currents at the Beaufort transect (moorings A, P, C and J) versus offshore distance; and (coherence)² between Beaufort sea level and longshore shelf currents at the Beaufort transect versus offshore distance; all at the coherent periods of 3.3, 5 and 10 d. Offshore distance is measured from the 28 m isobath.

the coast to the shelf break, top to bottom vertical density differences maintained at the shelf break by the adjacent ocean, heat exchange at the surface, and navifacial evaporation and precipitation.

We now consider the SAB and the upwelling mechanisms which exist there, and by implication, probably in other Western Boundary Current regions as well.

The South Atlantic Bight

The SAB, the southeastern-most coastline of the continental USA (Fig. 1.4), is characterized by a shallow, broad continental shelf. Shelf-break depths generally vary between 50–80 m and while the cross-shelf (or diabathic) width of the shelf proper is only about 25 km off both Cape Canaveral and Hatteras, the shelf is generally of the order of 100–150 km wide throughout the central portion of the SAB. To the north, there are three prominent coastal cusps, the Carolina Capes, which are partially separated from each other by extensive shoals. There are only minor land-derived freshwater sources in the Carolina Capes. In contrast, the Florida and Georgia coastlines comprise a curving land barrier characterized by low-lying swamps, tidal flats and several large rivers, which elicit substantial sources of freshwater to the shelf.

The SAB is graced by several persistent upwelling mechanisms: these include wind forcing, topographic effects, Gulf Stream frontal events and buoyancy flux influences. Thus, while the SAB does experience the more familiar, wind-driven phenomena of coastal upwelling, it also features several unusual but nontheless prominent and biologically, chemically and geologically important additional upwelling phenomena. The manner within which these upwelling phenomena manifest themselves will be presented in the following sections.

Wind-induced upwelling in the presence of a boundary current

Time and frequency domain intercomparisons of wind, coastal currents and coastal sea level in the SAB reveal a strong coupling between the longshore wind component and inner to mid-shelf currents and the rise and fall of the sea surface, in the two-day to two-week continuum of atmospheric forcing, and especially at the wind energy peak periods of 10, 5 and 3.3 days. Figure 1.5 depicts the coherency relationships between the longshore current component (V) with both the longshore wind stress component (τ^y) and coastal sea level (η), as measured from the 28 m isobath. Clearly at a distance of some 100 km from the coast (or 50 km from the 28 m isobath), in waters of approximately 45 m depth, the currents do not correlate well with either coastal winds or coastal sea level. However at a distance of 85 km from the coast (or 35 km from the 28 m isobath), in waters of <40 m depth, the correlation is excellent.

Chao & Pietrafesa (1980) and Weisberg & Pietrafesa (1983), both showed that the longshore wind stress (τ^y) is more energetic than the cross-shelf component (τ^x) in the Carolina Capes. Chao & Pietrafesa (1980) also showed that the effectiveness of τ^y in setting up both currents and coastal sea level is ten times greater than that of τ^x. These authors also found that the longshore wind stress component leads the coastal sea level response at Charleston by 8–9 h, however the cross-shelf sea level slope response to τ^y was found to be approximately 22 h. So, at the Charleston latitude, cross-shelf sea level gradients set up in an inertial period; which is the time required for the surface layer flow to be deflected to the right of the wind. A wind, τ^y, blowing parallel to the coast, is accompanied by a mass transport of magnitude τ^y/f (per unit width) directed perpendicular to the coast in a layer of thickness $D=\pi(2A/f)^{1/2}$, where f is the local Coriolis parameter and A is the vertical eddy viscosity coefficient. The cross-shelf sea surface slope can then be written as $\beta=2\pi^y/\rho gD$ and from geostrophy the alongshore slope current is $v=g\beta/f$. The time required for the slope current to be established is H/fD, where H is the total water depth. This scenario is found to be always true in 28 m of water, partially true in 40 m and occasionally true at 75 m. Inner-shelf waters of depth 28 m or less respond closely to the wind while those at 75 m rarely do so. At 40 m, response to the wind is evident but not primary.

Any scenario of a steady-state response to the longshore component of the wind in inner shelf waters in the SAB is convenient but overly simplistic. Mid- to inner shelf currents and

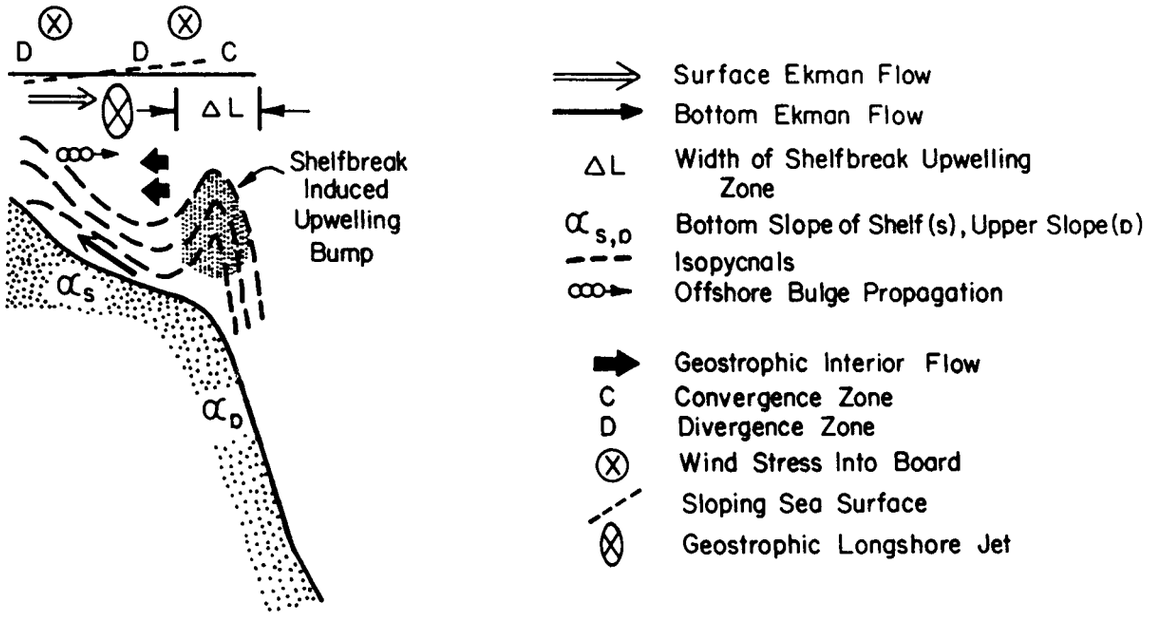

Fig. 1.6. Conceptual schematic of wind-induced upwelling processes in the South Atlantic Bight.

sea-level response to the wind have been described, documented and verified as time dependent responses to the total wind stress vector over variable topography by Chao & Pietrafesa (1980) and Janowitz & Pietrafesa (1980), respectively. Winds from the west to south quadrant cause sea level to fall at the coast while winds from the north to east quadrant cause a rise in sea level at the coast. Thus, a longshore wind directed to the northeast drives a surface layer offshore, which is initially balanced by an interior flow onshore and longshore. Within a day a bottom frictional layer becomes fully established and the flow within is directed onshore. Since this bottom layer is supplying mass, the interior flow drops off somewhat from its initial strength. A longshore jet is set up during this process. Since the shallow waters spin-up more rapidly, isopycnals appear to rise more quickly in shallow water. Actually, they simply have less vertical distance to traverse. The longshore jet has a negative cross-shelf gradient, i.e. its strength decreases with offshore distance (negative relative vorticity) and consequently the isopycnal rise process is suppressed. Since the spin-up process occurs first in shallower waters, the supression of the rise creates the impression of an isopycnal bulge moving from shallow to deeper waters. This process, shown pictorially in Figure 1.6, has been documented both theoretically and observationally by Janowitz & Pietrafesa (1980) to be the fundamental wind-induced upwelling process in the Carolina Capes. The terms in equations (1.1) and (1.2) considered by Janowitz & Pietrafesa (1980) to be of essential importance under conditions favorable for wind-driven upwelling are linearized (a), (b), (c) and (f) and linearized (g), (h), (i), and (l), respectively. This balance was confirmed by Purba (1984) for the Florida/Georgia region (the Georgia Bight) as well.

As shown in Figure 1.4, the mean alignment of the SAB is SSE–NNW from Cape Canaveral, Florida to New Brunswick, Georgia and southwest to northeast from Savannah, Georgia to Cape Hatteras, North Carolina. However there are also three cusps, the Carolina Cape bays, located in the northern half of the SAB. The coastal curvature is such that a favorable wind for upwelling can drive surface waters not only seaward but also against a northern boundary, such that sea level will rise in the direction of the wind and currents will be driven, geostrophically, in an interior cross-shelf flow directed to the left of the wind. This happens frequently in the northern halves of Long, Onslow and Raleigh bays (Askari, 1985).

In the southern end of the SAB, off Florida and Georgia, and in the southern half of the Carolina Cape bays, a northeastward wind which appears on the leading or eastern edge of an eastward moving low pressure weather system, a typical spring storm in the SAB (Weisberg & Pietrafesa, 1983), will drive surface waters offshore where the coastline is first encountered. Since the coastline is curved, the midpoint of the coastline will feel the wind first and consequently, sea level will fall at these midpoints earlier than to the north or south thereby creating a northward, longshore drop in sea level off Florida–Georgia and in the southern halves of the Carolina bays (Fig. 1.7). This drop will induce an offshore interior flow and decelerate the longshore jet. Thus in the southern part of the Georgia Bight and in the southern halves of the Carolina bays, compensatory flows are more confined to a bottom layer while in the northern part of the Georgia Bight and the bays the bottom flow is less intense since the interior onshore flow can supply the necessary mass.

Winds favorable for upwelling can occur any time of year on a transient basis (Fig. 1.8*a*) throughout the SAB and are especially persistent during spring and summer (Fig. 1.8*b*).

The degree to which the subinertial frequency time dependent response of the coastal ocean to atmospheric forcing is predicted by the theory of Janowitz & Pietrafesa (1980) can be tested by

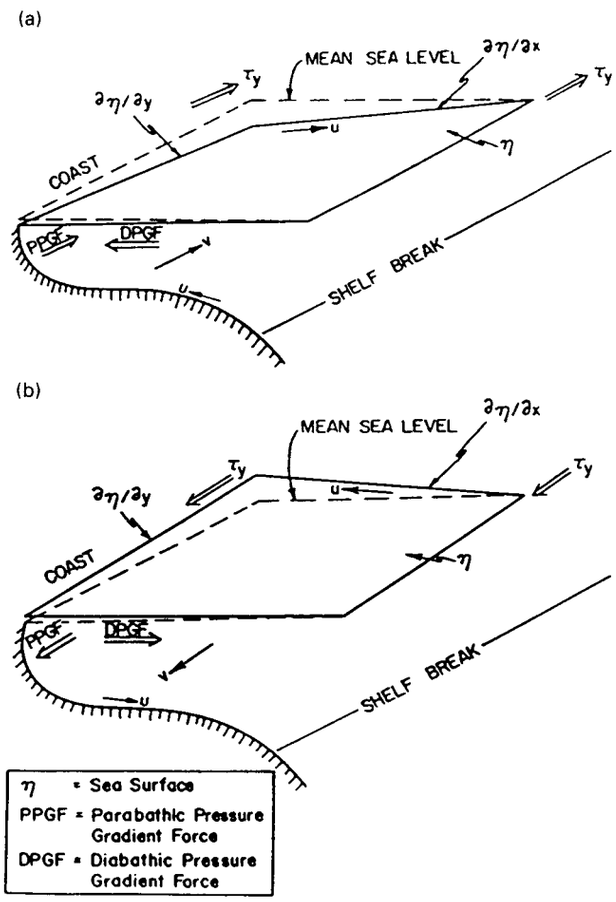

Fig. 1.7. Response of sea level to longshore wind stresses favorable for: (a) upwelling; and (b) downwelling in the southern halves of Raleigh and Onslow Bays, and from Cape Canaveral, Florida, to Charleston, South Carolina.

comparing longshore currents measured at a mooring site to those predicted by the model. Consider data acquired 12 m from the surface in 45 m of water at a mooring site located off Charleston, SC, for the 100-d period 13 April 1977–22 July 1977. The balance suggested by Janowitz & Pietrafesa (1980), states that the longshore wind-driven current is equal to the sum over time of the quantity defined as the difference between the magnitude of the observed longshore wind stress minus the square of the measured near bottom longshore velocity times a drag coefficient, all divided by the depth of the water column. In other words, the longshore wind-driven velocity is equal to the sum over time of the longshore wind stress minus the longshore component of bottom stress, all divided by depth. The cross-shelf velocity component is equivalent to the negative of the time rate of change of the longshore flow divided by the Coriolis parameter and the resulting vertical velocity is equal to the value of the depth multiplied by the offshore variation of the cross-shelf flow. These relationships are;

$$\frac{\partial v}{\partial t} = \frac{\tau^y - C_1 v}{h} \tag{1.8a}$$

$$u = -\frac{1}{f}\frac{\partial v}{\partial t} \tag{1.8b}$$

and

$$w = -z\frac{\partial u}{\partial x} \tag{1.8c}$$

where $C_1 = 0.01$, computed from observations. In the cross-shelf direction, the interior region is geostrophically balanced. We compare predictions of wind-driven longshore currents to measured longshore currents at a mid-shelf (40 m) interior station off Charleston in figure 1.9. The simple model misses the mark whenever Gulf Stream front waters are present such as model days 12–18, 32–46, and 70–76.

Thermohaline-driven upwelling

During late fall to early spring both momentum and buoyancy flux exchanges at the surface of the coastal ocean can drive coastal currents. During the fall, when cold air is suddenly advected offshore, the vertical density field is destabilized and vertical mixing ensues, creating a more vertically homogeneous density field. Atmospheric cold fronts tend to move offshore in the SAB, and as the advected cold air tends to equilibrium with the warmer coastal ocean by extracting heat, the surface waters are differentially cooled more quickly and efficiently at the surface and in shallower waters. This process has a destabilizing effect in the water column and the net result is that the isopycnals tend to slope downward in the offshore direction (ERT, 1979a). This negative slope of the diabathic density gradient effects a southward flow throughout the water column with the flow becoming increasingly southward with increasing depth, at a particular mooring location, relative to the surface flow. This process occurs via the thermal wind balance. It continues until late February to March and then reverses itself.

In the spring, warmer air begins to move offshore and the coastal ocean heats up, beginning in shallower waters. This process, in concert with an increase in fresh coastal water,

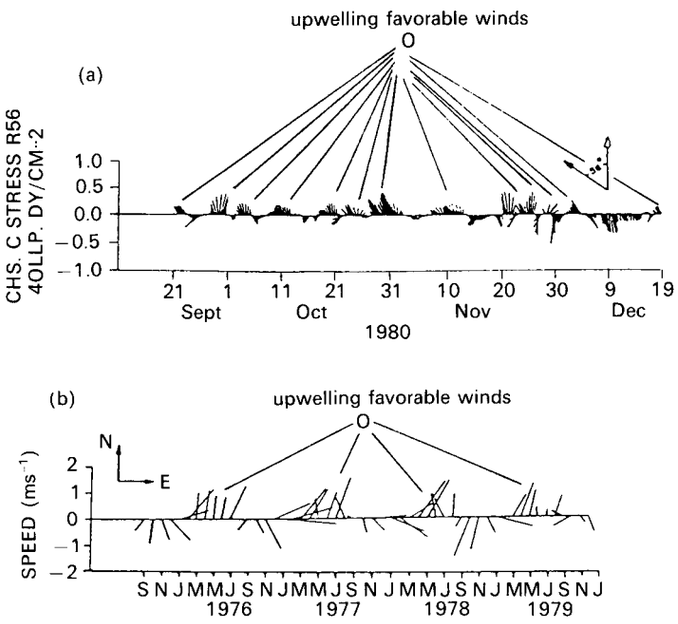

Fig. 1.8. Wind velocity vectors at the Charleston, South Carolina coastal station: (a) 40-hour low pass wind vectors; and (b) 30-day low pass wind vectors (adapted from Weisberg & Pietrafesa, 1983).

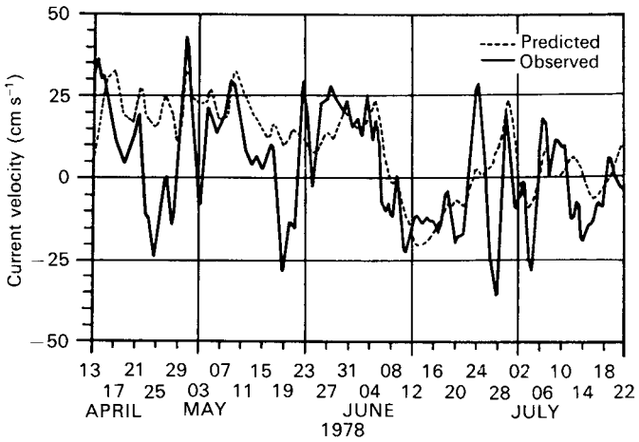

Fig. 1.9. Predicted versus observed mid-depth, longshore currents at a 40 m, mid-depth station, offshore of Charleston using the Janowitz–Pietrafesa (1980) model prediction.

derived from spring runoff, causes the isopycnals to slope downward toward the coast, supporting a northward flow in the water column. A flux across the shelf of heavy water can occur in spring in the SAB due to thermohaline forcing exacted from the positive salinity gradient set up by coastal waters made fresh by spring runoff and by the ever present highly saline Gulf Stream. Stommel & Leetma (1972) presented a theoretical analysis of circulation on a continental shelf under vertically homogeneous, horizontally stratified conditions. They considered a flat-bottomed, semi-infinite vertical plane shelf which was mechanically driven by surface winds and by a net input of freshwater, per unit length of coastline, along the surface. Stommel & Leetma's (1972) paper, the dissertations of Leetma (1969), Pietrafesa (1973) and the work of Pietrafesa & Janowitz (1979) are amongst the few which have dealt with thermohaline shelf forcing. The latter find that during the SAB spring transition period, freshwater runoff is at a maximum and forms a band of low salinity water near the coast, thus producing large cross-shelf salinity gradients. This effect combined with increased surface heating, which minimizes the shelf–Gulf Stream temperature differential, tends to produce maximum positive horizontal density gradients. Since this is also a period when vertical mixing begins to diminish because of a decrease in surface wind stress, a density-driven flow develops, which tends to stratify the shelf. Lighter (fresher) water, moves offshore on the surface and denser (saltier) water intrudes onshore along the bottom. This spring intrusion may also upwell cooler, deeper Gulf Stream waters having higher nutrient content onto the shelf for subsequent biological uptake. Both the drifter results of Bumpus (1973) and the averaged current meter data (fig. 1.10) indicate onshore bottom flows for this period. Summer heating and diminished vertical mixing tend to increase the temperature contrast in the stratified layers.

For the winter period in the Mid-Atlantic Bight shelf region, Stommel & Leetma (1972) found an approximate functional dependence of the salt penetration scale across the shelf (L) on the Ekman number (E) and wind stress τ. Here the salt penetration scale is defined as: $L = So/(\partial S/\partial X)$ and the vertical Ekman number as $E = A/fH^2$, where So is the mean salinity, X is in the cross-shelf direction, A is the vertical eddy viscosity, f is the Coriolis parameter and H is water depth. As E becomes small, L increases and depends mainly on the wind stress. Also, along-shelf winds appear to have more influence on the salt penetration distance than do cross-shelf winds. As the depth becomes shallow, mixing increases. The available salt is thus mixed with the subsurface water, decreasing both the transport of salt onshore and the values of L. We have taken the liberty of recalculating the Stommel & Leetma estimate by deriving exact solutions and find that (Fig. 1.11) density driving, while generally less effective than wind forcing in moving heavy bottom water across the shelf, nontheless is capable of transporting such waters from the shelf break across the width of most of the SAB shelf. For example thermohaline forcing can drive salt across a shelf of width 10^7–10^8 km, more effectively than can a 1 dyne/cm^2 wind stress directed either shoreward or with the coast to its right for vertical Ekman numbers of .02–1.

Climatological distributions of salinity presented by Atkinson *et al.* (1982) suggest that low salinity water is carried northward and offshore in spring and southward against the coast in autumn. During April and May surface water with salinity < 36 ppt is found along the shelf break between 32 and 33° N. This water is clearly a mixture of low salinity inner shelf and Gulf Stream water. According to Blanton & Atkinson (1983), the evacuation of low salinity water adjacent to the Georgia coast occurs most rapidly in spring just after river discharge reaches a maximum. The rate of evacuation is very likely related to the strength and persistence of the longshore wind stress. The water in the upper layers of the inner shelf frontal zone is likely carried northward with a strong offshore component such that low salinity water originally present in surface layers adjacent to the Georgia (and probably South Carolina) coast is advected toward the outer shelf between 32 to 33° N. The coupling of two upwelling driving mechanisms, wind stress and buoyancy stress during spring leads to replenishment

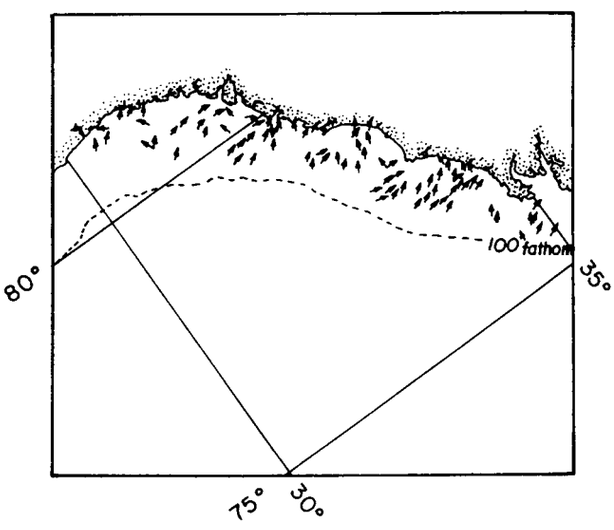

Fig. 1.10. Near-bottom current vector means for late March, April, May and early June as inferred from 10 years of bottom drifter data (Bumpus, 1973) and moored current meter data.